JIM Vol.8 (1) 2026

Received: 05 02 2026 | Revised:10 03 2026 | Accepted: 15 04 2026

DOI: 10.15294/jim.v8i1.42395

Page 9 - 17

JIM: Jurnal Inovasi Mesin

Mechanical Integrity Verification of Atmospheric Sump Tanks under Sustained Hydrostatic Loading in Fuel Pipeline Facilities

Farand Putra Hendratmo[1], Muhammad Ritzky Novhar[2], Dharu Feby Smaradhana[1*]

1 Department of Mechanical Engineering, Faculty of Engineering, Universitas Sebelas Maret, Surakarta, Indonesia
2 Mechanical Engineering, Engineering Department, PT. Pratiwi Putri Sulung, Bekasi, Indonesia

*dharufs@staff.uns.ac.id

Keywords:
Atmospheric sump tank
Hydrostatic loading
Mechanical integrity
Nozzle reinforcement
Pressure

Abstract

Atmospheric sump tanks are commonly classified as low pressure equipment; however, when operated under sustained liquid filled conditions, their mechanical integrity may be governed by localized structural mechanisms rather than global shell membrane capacity. This study presents a calculation based mechanical integrity verification of a horizontal atmospheric sump tank subjected to sustained hydrostatic loading. The methodology integrates a hydrostatic pressure model with a specific gravity consistency check derived directly from the applied liquid head, and a component-based capacity evaluation performed using effective corroded thickness. The sustained design pressure (combining atmospheric base and hydrostatic head) is established as 1.135 bar (absolute), while the maximum allowable working pressure (MAWP) is evaluated for shell, heads, and nozzle discontinuities. Results indicate that while the global shell capacity is high, the integrity is governed by nozzle reinforcement limits, yielding a governing MAWP of 2.954 bar (gauge equivalent). Sensitivity analysis on fuel specific gravity demonstrates that reasonable density variations affect pressure demand magnitude but do not alter the governing capacity mechanism. Hydrostatic test pressure is subsequently verified using allowable stress scaling, yielding a test pressure of 3.840 bar. The findings demonstrate that integrity verification of atmospheric sump tanks under sustained hydrostatic loading must prioritize local discontinuity-controlled capacity and physically consistent demand modelling rather than pressure only membrane stress assumptions.

1 Introduction

Atmospheric storage tanks and sump tanks are critical assets in fuel transportation and distribution systems. Although they operate at nominally low pressures, thin-walled shell structures subjected to liquid loading can fail through mechanisms not governed by membrane stress alone, including local yielding, geometric instability, and stress concentration at structural discontinuities. Prior studies have shown that global shell behaviour may remain elastic while localized regions reach critical stress states due to openings, imperfections, and boundary constraints [1,10]. Therefore, integrity assessment of atmospheric tanks requires a mechanics-based approach beyond simplified pressure checks.

Existing research has predominantly addressed vertical tanks, emphasizing buckling under wind, vacuum, seismic excitation, and settlement. Godoy highlighted that buckling resistance is highly sensitive to imperfections and boundary conditions even when stresses are well below material strength limits [10], consistent with later numerical and experimental evidence showing that non-uniform loading and constrained supports promote local failure modes [11,12]. In parallel, integrity assessment practice

ISSN 2746-7694

increasingly incorporates realistic geometry and degradation: laser-scan characterization combined with nonlinear finite element analysis can change predicted stress/strain distributions and reveal governing

failure mechanisms overlooked by nominal design [1], while fitness for service evaluations confirm that dents/distortions can control acceptance despite adequate global capacity [2,3]. Corrosion reduces effective thickness and alters stress redistribution, requiring coupled treatment of inspection data, corrosion modeling, and mechanical verification [4-6]; welding residual stresses and fabrication effects may further intensify local stress concentration and crack initiation [13].

Despite this extensive literature, horizontal atmospheric sump tanks under sustained hydrostatic loading have received limited attention. Unlike vertical tanks, horizontal sump tanks experience asymmetric hydrostatic pressure distribution, liquid weight effects, and strong interaction with saddle supports, producing combined membrane bending responses. Sustained hydrostatic loading may activate governing mechanisms different from transient conditions, particularly when local discontinuities exist [16]. Moreover, nozzles and manways impose reinforcement requirements that may govern maximum allowable working pressure (MAWP) long before global shell capacity is reached [7,15]. While standards provide general inspection and assessment guidance [8,9], they do not explicitly address mechanics driven identification of governing capacity mechanisms for sump tanks under prolonged hydrostatic head.

Accordingly, this study presents a mechanics-based integrity verification of an atmospheric sump tank subjected to sustained hydrostatic loading. The work integrates hydrostatic load modelling, a specific gravity consistency checks derived from the applied liquid head, and component level capacity evaluation to identify the governing structural mechanism. By clarifying the interaction between global shell response and reinforcement controlled local capacity, this study contributes a physically grounded integrity framework for atmospheric sump tanks operating under sustained liquid filled conditions in fuel pipeline facilities.

2 Methodology

This study adopts a mechanics governed, calculation-based integrity verification framework to assess the structural behavior of a horizontal atmospheric sump tank subjected to sustained hydrostatic loading. The methodology is formulated to ensure that the governing integrity mechanism is identified based on physical load resistance consistency, rather than compliance-oriented pressure checks. Emphasis is placed on transparent derivation of demand, conservative representation of resistance, and explicit identification of the component controlling structural integrity, in line with established practices in storage tank mechanics and fitness for service assessment [1-3,6,9].

Figure 1 illustrates the component-based integrity verification framework adopted in this study, emphasizing the sequential evaluation of load demand and structural resistance to identify the governing pressure limiting mechanism. The figure clarifies that integrity is determined by the most critical component rather than by global shell behavior alone.

Figure 1. Component based integrity verification framework

2.1 Structural Configuration, Material Properties, and Degradation Representation

The investigated sump tank is modelled as a thin-walled cylindrical shell equipped with ellipsoidal end heads, multiple nozzles, and saddle type supports. This structural configuration is representative of atmospheric sump tanks commonly used in fuel handling systems, where the mechanical response is governed by the interaction of internal pressure, liquid weight, support reactions, and local structural discontinuities [1,10].

Material properties correspond to pressure vessel grade carbon steel typically employed in atmospheric storage tanks. To account for in service degradation and to ensure conservative capacity estimation, structural resistance is evaluated using an effective corroded thickness, defined as Eq. (1).

$$t_{eff} = t_{nom} - CA \tag{1}$$

where t_{nom} is the nominal plate thickness and CA is the corrosion allowance. The adoption of effective thickness ensures that the integrity assessment reflects the most critical credible operating condition and is consistent with degradation aware integrity and fitness for service methodologies [6,9].

Table 1 summarizes the complete geometric, material, and mechanical parameters used in the integrity verification. All pressure capacity and hydrostatic test evaluations are consistently based on the effective corroded thickness and sustained design pressure defined in this table.

Table 1. Design geometry, material properties, and mechanical parameters used in the integrity verification

Parameter	Symbol	Value
Internal diameter of shell	D	1600 mm
Radius	R	800 mm
Straight shell length	L	2785 mm
Nominal thickness	t_{nom}	10 mm
Corrosion allowance	CA	3 mm
Effective thickness	t_{eff}	7 mm
Head type	–	2:1 Ellipsoidal
Material type	–	Carbon steel
Allowable stress (55 °C)	S	138 MPa
Allowable stress ratio	$\frac{Sa}{S}$	1.0
Joint efficiency	E	1.0
Support type	–	Two saddles
Base internal pressure	P_{base}	1.000 bar
Hydrostatic head pressure	P_{head}	0.135 bar
Sustained design pressure	P_{design}	1.135 bar

2.2 Sustained Hydrostatic Loading and Pressure Distribution

The critical loading scenario considered in this study is sustained hydrostatic loading, corresponding to prolonged liquid filled conditions. Sustained loading differs fundamentally from transient filling or hydrostatic testing, as it produces steady state stress fields that may activate local integrity controlling mechanisms over extended durations [16].

The internal pressure acting on the tank wall is modeled as the superposition of a base internal pressure and a depth dependent hydrostatic component as seen in Eq. (2).

$$P_{design} = P_{base} + P_{head} \tag{2}$$

Assuming the tank is vented or operates at near-atmospheric conditions, the base pressure P_{base} is taken as 1.0 bar (absolute). Consequently, the structural verification considers the differential pressure governed by the hydrostatic head, effectively modeled as gauge pressure for code compliance checks. The hydrostatic pressure distribution is defined by Eq. (3).

$$p(z) = \rho g z \tag{3}$$

where ρ is the fluid density, g is gravitational acceleration, and z is the vertical coordinate measured from the liquid free surface. This formulation captures the linear pressure gradient inherent to liquid storage systems and has been widely adopted in mechanics-based analyses of storage tanks [10-12].

The resulting sustained design pressure is $P_{\text{design}} = 1.135$ bar. The physical interpretation of this pressure gradient and its interaction with saddle supports are illustrated in Figure 2, which presents a preliminary Finite Element Analysis (FEA) solely to illustrate the stress distribution concept. However, the verification in this study strictly follows standard analytical code calculations to ensure regulatory compliance.

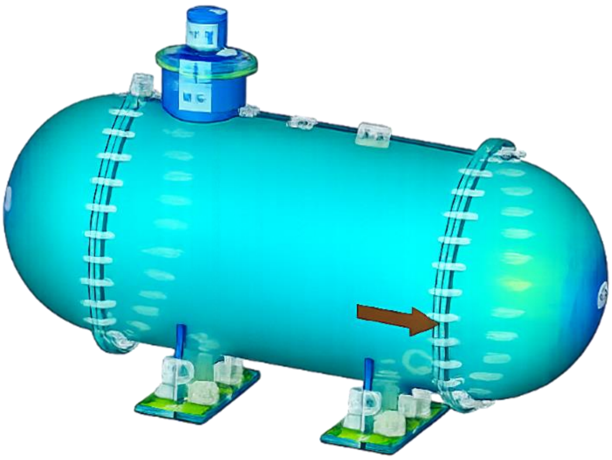

Figure 2. Hydrostatic pressure distribution under sustained loading

2.3 Specific Gravity Consistency Verification

In practical engineering applications, the specific gravity of the contained fluid is not always explicitly defined. To avoid introducing arbitrary assumptions, this study performs a specific gravity consistency verification, whereby the fluid density is inferred directly from the applied hydrostatic head. Using the hydrostatic relation in Eq. (4).

$$p = \rho g h \tag{4}$$

and the specified hydrostatic pressure increment of 0.135 bar at a representative liquid height of approximately 1.6 m, the implied fluid density is calculated as approximately 860 kg/m³, corresponding to a specific gravity of 0.86. This value is consistent with typical fuel properties encountered in pipeline and storage systems [6,16].

To evaluate the robustness of the integrity conclusions, bounding values of specific gravity are also considered. These cases, summarized in Table 2, represent the specific gravity bounds considered in the analysis and the resulting hydrostatic pressure contribution.

These cases are used to assess the sensitivity of sustained pressure demand to plausible variations in fuel density. As demonstrated later in the Results section, these variations influence pressure demand magnitude but do not alter the governing structural mechanism.

Table 2. Specific gravity bounds and corresponding hydrostatic pressure for sustained loading

Case	Specific Gravity (SG)	Fluid Density	Hydrostatic Head Pressure	Sustained Design Pressure
Lower bound	0.80	800 kg/m³	0.125 bar	1.125 bar
Base case	0.86	860 kg/m³	0.135 bar	1.135 bar
Upper bound	0.90	900 kg/m³	0.141 bar	1.141 bar

2.4 Component Capacity Assessment and Governing Mechanism Identification

Structural capacity is evaluated using a component-based assessment approach, acknowledging that different tank elements may govern integrity under sustained hydrostatic loading. This framework is particularly essential for thin-walled shell structures containing openings, where localized behavior frequently controls acceptability even when global capacity remains adequate [1-3]. The assessment is conducted sequentially by first evaluating the global capacity of the shell and head using thin-shell pressure relations together with the effective corroded thickness, followed by evaluation of local capacity at structural discontinuities especially nozzle regions through reinforcement adequacy criteria that explicitly account for stress concentration and load redistribution, and finally identifying the governing maximum allowable working pressure (MAWP) as the minimum allowable pressure among all evaluated components. The hierarchical nature of this verification is illustrated in Figure 1, emphasizing that integrity limits may be controlled by localized, reinforcement-governed mechanisms even when global shell stresses remain well below material strength limits.

2.5 Hydrostatic Test Pressure Evaluation

Hydrostatic test pressure is evaluated to verify structural integrity beyond normal operating conditions and to establish an additional verification envelope. The test pressure is determined using allowable stress scaling relative to the governing MAWP in Eq. (5).

$$P_{test} = 1.3 \times MAWP \times \frac{Sa}{S} \quad (5)$$

where S and S_a are the allowable stresses at operating and test temperatures, respectively. This formulation ensures consistency between operating and test conditions and aligns with established pressure vessel practice [9,16].

The parameters used in the hydrostatic test pressure evaluation and the resulting test pressure are reported in Table 4, providing transparency and reproducibility of the verification procedure.

2.6 Methodological Scope and Applicability

The proposed methodology integrates physically consistent hydrostatic load definition, degradation aware resistance representation, and component-based capacity evaluation into a unified integrity verification framework. While the present study focuses on calculation-based assessment, the framework is fully compatible with future extensions incorporating numerical simulation or inspection derived geometric data, as demonstrated in recent tank integrity studies [1-5].

3 Results and Discussion

3.1 Governing Pressure Capacity under Effective Corroded Condition

The calculated pressure capacities indicate a clear separation between global shell resistance and local reinforcement-controlled resistance. Under the effective corroded thickness condition, the cylindrical shell and ellipsoidal heads exhibit high allowable pressure capacity when evaluated using thin-walled shell relations. However, this global capacity does not govern the allowable operating limit of the sump tank.

The component based maximum allowable working pressure (MAWP) values are summarized in Table 3. The table shows that the governing MAWP of the tank is 2.954 bar, which is controlled by nozzle reinforcement capacity. This value is substantially lower than the pressure capacity associated with the shell and heads, demonstrating that the integrity limit is governed by localized structural behavior rather than by global membrane stress. It is noted that the nominal thickness of 10 mm is relatively high for typical atmospheric service. This thickness provides significant global membrane capacity, as evidenced by the high shell MAWP (11.82 bar). However, this 'over design' in the shell highlights the criticality of the nozzle reinforcement, which remains the weakest link despite the robust shell construction

Table 3. Summary of MAWP values and governing component (corroded condition)

Component	Governing criterion	MAWP
Cylindrical shell	Circumferential membrane stress	11.82 bar
Ellipsoidal heads	Membrane stress	9.40 bar
Nozzle reinforcement	Reinforcement adequacy	2.954 bar

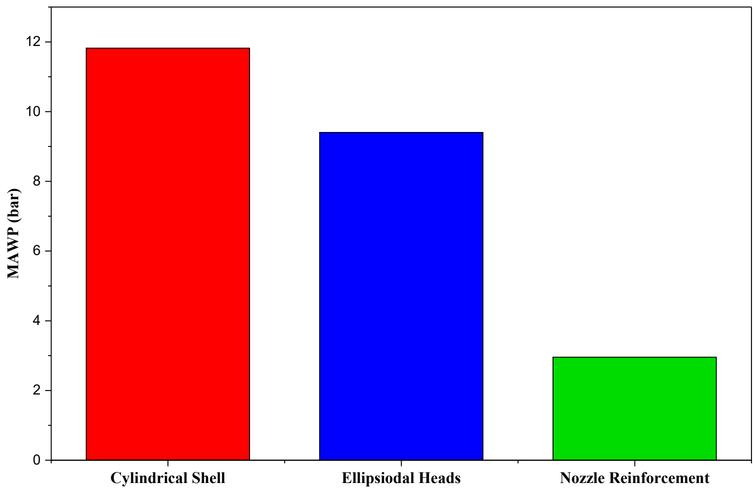

Figure 3. Comparison of component MAWP values

The hierarchy of component capacities is illustrated in Figure 3, which compares the MAWP values of shell/head components and reinforcement-controlled components. The figure confirms that reliance on shell membrane capacity alone would not identify the governing integrity limit, as local discontinuity behavior reaches its allowable condition first. From a mechanical perspective, this result is consistent with established behavior of thin-walled shell structures containing openings, where stress concentration and load redistribution around penetrations control allowable pressure even when global stresses remain moderate.

3.2 Response under Sustained Hydrostatic Loading

The sustained design pressure, including the hydrostatic contribution, is calculated as 1.135 bar. Comparison of this pressure with the governing MAWP of 2.954 bar shows that the operating condition remains well within the allowable capacity envelope.

To examine the influence of fluid properties, the specific gravity bounds defined in Table 2 are applied. An increase in specific gravity results in a proportional increase in hydrostatic pressure demand. However, across all examined cases, the sustained hydrostatic pressure remains significantly lower than the governing MAWP. This result demonstrates that while fluid density affects the magnitude of hydrostatic loading, it does not change the governing structural mechanism. The mechanical integrity of the sump tank under sustained hydrostatic loading is therefore insensitive to reasonable variations in fuel density, provided that local reinforcement capacity remains unchanged.

3.3 Hydrostatic Test Pressure Verification

Hydrostatic test pressure is evaluated as an additional integrity verification beyond normal operating conditions; by applying allowable stress scaling relative to the governing MAWP, the hydrostatic test pressure is calculated as 3.840 bar, with the calculation parameters and resulting value summarized in Table 4 to ensure transparency and reproducibility. The relationship between sustained design pressure, governing MAWP, and hydrostatic test pressure is further illustrated in Figure 4, which presents the pressure hierarchy adopted in this study and demonstrates that the sustained design pressure is bounded by the governing MAWP and subsequently verified through hydrostatic testing, thereby confirming the consistency of the defined integrity envelope.

Table 4. Hydrostatic test pressure evaluation based on governing MAWP

Parameter	Value
Governing MAWP	2.954 bar
Sustained design pressure	1.135 bar
Test pressure factor	1.3
Allowable stress ratio $\left(\frac{Sa}{S}\right)$	1.0
Hydrotest pressure	3.840 bar

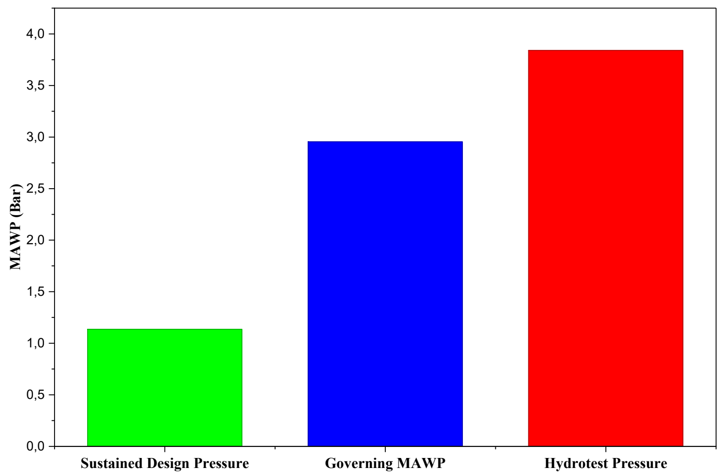

Figure 4. Pressure hierarchy for integrity verification

3.4 Discussion of Governing Mechanical Behavior

The results demonstrate that the mechanical integrity of the atmospheric sump tank under sustained hydrostatic loading is governed by local nozzle reinforcement capacity, rather than by global shell membrane behavior. Although the shell and heads retain sufficient pressure resistance, the presence of openings introduces localized stress concentration that limits the allowable pressure. This finding confirms that integrity verification of atmospheric sump tanks cannot rely solely on global shell checks or nominal pressure classification. Instead, component-based evaluation is required to identify the true governing mechanism under sustained hydrostatic loading. The consistency of the governing mechanism across all examined specific gravity cases further confirms that the adopted hydrostatic loading model is physically coherent and that the identified integrity limit is robust with respect to plausible operating variations.

3.5 Practical Implications

The identification of nozzle reinforcement as the governing component has direct implications for integrity verification and maintenance practice. Inspection and assessment efforts should prioritize local discontinuity regions, particularly nozzle reinforcement and associated welds, rather than focusing exclusively on shell thickness or global pressure limits. For integrity evaluation of similar atmospheric sump tanks, the results highlight the importance of using calculation based, component level verification frameworks to ensure that localized governing mechanisms are correctly identified.

3.6 Safety Factor Evaluation

To explicitly quantify the structural safety margin, a utilization-based safety factor evaluation is performed by comparing the sustained operating pressure with the governing MAWP. The utilization ratio (UC) is defined as the ratio between actual operating pressure and allowable pressure capacity in Eq. (6).

$$UC = \frac{P_{operating}}{MAWP} \tag{6}$$

Using the sustained design pressure of 1.135 bar and the governing MAWP of 2.954 bar, the calculated utilization ratio is 0.384, corresponding to a safety factor of approximately 2.60. This result indicates that the sump tank operates at less than 40% of its governing allowable pressure capacity under sustained hydrostatic loading.

From a mechanical perspective, the relatively low utilization ratio confirms that the governing nozzle reinforcement operates well within the elastic regime, with sufficient margin against yielding or reinforcement inadequacy under long term hydrostatic loading. Importantly, this safety margin is achieved despite the integrity being controlled by a localized structural feature, highlighting that local discontinuity-controlled behaviour does not necessarily imply marginal safety when properly evaluated using calculation-based methods. Based on the calculations performed, it can therefore be concluded that the proposed sump tank design is structurally valid and exhibits a conservative integrity margin under sustained operating conditions.

4 Conclusions

This study presents a mechanics-based integrity verification of an atmospheric sump tank subjected to sustained hydrostatic loading by integrating physically consistent load definition, degradation aware resistance representation, and component level capacity evaluation. The analysis demonstrates that, despite the low nominal operating pressure, the governing integrity mechanism is controlled by localized nozzle reinforcement capacity rather than by global shell membrane resistance, with a governing maximum allowable working pressure (MAWP) of 2.954 bar. The sustained design pressure of 1.135 bar is significantly lower than this governing capacity, resulting in a utilization ratio (UC) of 0.384, which corresponds to a safety factor of approximately 2.60. This quantitative safety margin confirms that the proposed sump tank design operates well within its allowable pressure envelope under sustained hydrostatic conditions. Verification at the hydrostatic test pressure of 3.840 bar further supports the consistency of the integrity envelope associated with the governing component. The findings highlight the limitations of pressure only assessment approaches for atmospheric tanks and emphasize the necessity of calculation-based, component level verification frameworks that explicitly identify localized, reinforcement-controlled integrity mechanisms. Overall, the proposed methodology provides a transparent, systematic, and reproducible basis for reliable integrity assessment of atmospheric sump tanks, with particular relevance for engineering practice focused on critical local structural features under sustained liquid filled operation.

References

1. M. A. Lopes, F. J. C. P. Soeiro, and J. G. S. Silva, "Nonlinear buckling behavior and stress and strain analyses of atmospheric storage tank aided by laser scan dimensional inspection technique," *Journal of the Brazilian Society of Mechanical Sciences and Engineering*, vol. 44, art. 443, 2022, doi: 10.1007/s40430-022-03752-z.
2. W. Herucakra and L. P. Adnyani, "Integrity Assessment of Dented Aboveground Steel Storage Tank After Hydrostatic Testing," *International Journal of Marine Engineering Innovation and Research*, vol. 10, no. 2, pp. 387–396, 2025.
3. W. Herucakra, L. P. Adyani, I. C. F. H. Prasetyo, and A. R. Rizkhita, "Fitness for Service (FFS) and Fatigue Assessment for Shell Distorted Steel Storage Tank Based on API 579-1/ASME FFS-1," *Journal of Materials Exploration and Findings*, vol. 3, no. 1, pp. 1–8, 2024.
4. A.-A. Stoicescu, R. G. Ripeanu, M. Tănase, and L. Toader, "Current Methods and Technologies for Storage Tank Condition Assessment: A Comprehensive Review," *Materials*, 2024.
5. A.-A. Stoicescu, R. G. Ripeanu, M. Tănase, C. N. Ilincă, and L. Toader, "Multifactorial Analysis of Defects in Oil Storage Tanks: Implications for Structural Performance and Safety," *Processes*, 2025.
6. Y. Feng, Y. Yang, and B. Huang, "Corrosion analysis and remaining useful life prediction for storage tank bottom," *International Journal of Advanced Robotic Systems*, pp. 1–9, 2019, doi: 10.1177/1729881419877051.
7. M. J. Shirshahi, S. F. Chini, P. Taheri, and A. Mansouri, "A comparative numerical evaluation of linear anode arrangements for enhancing above ground storage tank cathodic protection via mesh grid and concentric ring designs," *Scientific Reports*, 2023.
8. API, *API Standard 653: Tank Inspection, Repair, Alteration, and Reconstruction*, 3rd ed., 2001 (Addendum 1, 2003).
9. ASME**,** *ASME Boiler and Pressure Vessel Code, Section VIII: Rules for Construction of Pressure Vessels, Division 1*, New York: American Society of Mechanical Engineers, 2023.
10. L. A. Godoy, "Buckling of vertical oil storage steel tanks: Review of static buckling studies," *Thin-Walled Structures*, vol. 103, pp. 1–21, 2016.
11. E. Brunesi and R. Nascimbene, "Evaluating the Seismic Resilience of Above-Ground Liquid Storage Tanks," *Buildings*, 2024.
12. R. Zhang, S. Chu, K. Sun, Z. Zhang, and H. Wang, "Effect of the Directional Components of Earthquakes on the Seismic Behavior of an Unanchored Steel Tank," *Applied Sciences*, 2020.
13. G. Wu et al., "Control of Welding Residual Stress in Large Storage Tank by Finite Element Method," *Metals*, vol. 12, art. 1502, 2022, doi: 10.3390/met12091502.
14. Y. Jiao et al., "Finite Element Analysis and Improved Evaluation of Mechanical Response in Large Oil Storage Tanks Subjected to Non-Uniform Foundation Settlement," *Processes*, 2024.
15. R. Safaeian, R. Sharifi, A. Dolati, and S. Medhat, "Analyzing and design of mesh ribbon cathodic protection for aboveground storage tanks," *South African Journal of Chemical Engineering*, vol. 45, pp. 51–59, 2023.
16. H. S. da Costa Mattos, L. M. Paim, and J. M. L. Reis, "Analysis of burst tests and long-term hydrostatic tests in produced water pipelines," *Engineering Failure Analysis*, vol. 22, pp. 128–140, 2012.